Coastal gradients in False Bay, south of Cape Town: what insights can be gained from mesoscale reanalysis?

Mark R Jury

Geography Dept, Univ Zululand, South Africa

and Physics Dept, Univ Puerto Rico Mayaguez, USA

Abstract

Mesoscale datasets are used to study coastal gradients in the marine climate and oceanography in False Bay, south of Cape Town. Building on past work, satellite and ocean / atmosphere reanalysis are used to gain new insights on the mean structure, circulation and meteorological features. HYCOM v3 hindcasts represent a coastward reduction of mixing that enhances stratification and productivity inshore. The mean summer currents are westward –.4 m/s along the shelf edge and weakly clockwise within False Bay. The marine climate is dominated by southeasterly winds that accelerate over the mountains south of Cape Town and fan out producing dry weather. Virtual buoy time series in Dec 2012-Feb 2013 exhibit weather-pulsed upwelling in early summer interspersed with quiescent spells in late summer. Intercomparisons between model, satellite and station data build confidence that coupled reanalyses yield opportunities to study air-sea interactions in coastal zones with complex topography. The 0.083° HYCOM reanalysis has 16 data points in False Bay~~the embayment south of Cape Town~~, just adequate to resolve the coastal gradient and its impacts on ocean productivity.

mark.jury@upr.edu

Introduction

The coastal zone south of Cape Town, South Africa is comprised of linear sandy beaches and a semi-enclosed bay surrounded by mountains (Fig 1a,b). False Bay is southward facing and about 10^3 km^2, with the Cape Peninsula to the west and Cape Hangklip to the east. The shelf oceanography exhibits a range of conditions from seasonally pulsed upwelling events (Shannon and Field 1985, Lutjeharms and Stockton 1991, Largier et al. 1992, Dufois and Rouault 2012) to warm-water intrusions from the Agulhas Current, creating great biological diversity (Shannon et al 1985, Griffiths et al. 2010). The upper ocean circulation tends to be northwestward and pulsed at subseasonal time scales by passing weather, shelf waves, warm rings and tides (Grundlingh and Larger 1991; Nelson et al. 1991). Coastal winds and temperatures exhibit sharp ~~cross-shelf~~ gradients (Bang 1971, Jury 1991, VanBallegooyen 1991) depending on excursions ~~latitude fluctuations~~ of the subtropical anticyclone.

The high pressure cells of the South Atlantic and South Indian Ocean tend to join in summer and produce dry weather and upwelling-favourable winds from the southeast that are shallow and diverted around the >1000 m mountains of Cape Hangklip and the Cape Peninsula (Fig 1a,b). The winds accelerate off the capes and form shadow zones over leeward bays, creating cyclonic vorticity that enhances upwelling (Wainman et al. 1987, Grundlingh and Largier 1991, Jacobson et al. 2014). Winds entering False Bay become channeled N-S and tend to induce standing clockwise rotors in the upper ocean (deVos et al. 2014), which are pulsed by geostrophic currents across the mouth.

With the passage of eastward-moving atmospheric Rossby waves across the southern tip of Africa at 3-20 day intervals (Jury and Brundrit 1992), the subtropical ridge is replaced by coastal lows followed by downwelling-favourable northwesterly winds and frontal troughs that bring rainfall, stormy seas, onshore transport and mixing – most often in winter: May-Sep, (Engelbrecht et al. 2011, Schilperoort et al. 2013, deVos et al. 2014, Rautenbach 2014).

The city of Cape Town, its 4 million residents (Statistics SA 2020) and associated infrastructure have intensified anthropogenic pressure on the ~~southern~~ coastal zone. Sandy beaches there are vulnerable to sediment loss from rising seas, huge swell events and recreational use (Mather et al. 2009, Theron et al. 2010; Roux & Toms 2013, Theron et al. 2014, Fourie et al. 2015). Climate-change has become manifested in longer summers and a southeastward shift in wind-driven upwelling, marine ecosystems and fisheries (Rouault et al. 2010, Lloyd et al. 2012, Blamey et al. 2012, Schlegel et al. 2017).

Coastal embayments tend to be very productive and False Bay is no exception. Brown et al. (1991) reported an average chlorophyll concentration of 4 mg m^{-3} in the euphotic layer, that varies from summer to winter: 5.5 vs 2.1 mg m^{-3} (Giljam 2002). Nutrients enter the southern coastal zone via runoff and municipal waste streams (Parsons 2000, Taljaard et al. 2000). Although numerous small rivers drain into False Bay, the nutrients supplied by upwelling exceed those from terrestrial sources (Taljaard 1991, Giljam 2002). Coastal and offshore waters show healthy rates of exchange, particularly during stormy spells that induce surf-zone currents and a dissipation of the thermocline.

Our understanding of the physical oceanography south of Cape Town has benefited from studies of the upper ocean circulation (Botes 1988), the wind field and the variability of sea temperatures (Dufois et al. 2012). Yet many processes governing intra-seasonal variability remain obscure (Wainman et al. 1987). There is a lack of consensus on the mean seasonal circulation (Grundlingh et al. 1989, Taljaard et al. 2000), despite ample knowledge of the air-sea interactions. To overcome the limited scale and brevity of measurement campaigns, modelling efforts (eg. Penven et al. 2001) have elucidated coastal features over a longer period. Hydrodynamic simulations with temporal forcing by Nicholson (2011) gave promising results, and Coleman (2019) recently modelled the circulation south of Cape Town forced with daily data from the Hybrid-Coordinate Ocean Model (HYCOM; Cummings and Smedstad 2013) and the Weather Research and Forecasting model (WRF; Skamarock et al. 2008). Coleman (2019) found sheared clockwise circulations during summer, and favourable validations for mean currents and thermal stratification in False Bay.

Given the above history of scientific endeavors, the objective of this work is to embark on a new mission to utilize the global ocean data assimilation system to describe the spatial pattern and temporal variability of the marine environment. We demonstrate that mesoscale reanalysis offers valuable new insights on the coastal gradient in summer climate and physical oceanography south of Cape Town.

Data

Marine climate variability is described using weather and wave reanalysis products at 20-30 km resolution, namely CFSr2, ECMWF, Wavewatch3 (Saha et al. 2014, Dee et al. 2011, Tolman 2002; respectively). Coastal gradients are described using 4 km resolution satellite visible and infrared products (Reynolds et al. 2002), and IMT station observations in western False Bay. Table 1 lists acronyms and dataset attributes.

The mesoscale oceanography of False Bay, south of Cape Town is studied with HYCOM v3.1 reanalysis (Cummings and Smedstad 2013; Metzger et al. 2014), that assimilates microwave, infrared and visible measurements from multiple satellites, calibrated with in-situ observations. Climatology, persistence and model-calculated fields are used to quality-control and nudge the incoming data, within static 0.033° resolution GIS fields that include bathymetry, surface roughness, etc. Running in parallel with the ocean model are operational atmosphere and land models that deliver coupled information on momentum, heat and water fluxes and feedbacks (Table 1). In the 41-layer 0.083° HYCOM v3.1 hindcast employed here, Navgem v1.4 3-hourly 0.176° resolution atmospheric data provide background initialization for kinematic and thermodynamic fields derived from satellite and insitu measurements, continually assimilated over a rolling 5-day window (Hurlburt et al. 2009). A hydrological submodel assimilates satellite rainfall / soil moisture and predicts runoff, which is blended with satellite salinity measurements (Table 1). Regional v~~V~~alidations have been done for the HYCOM reanalysis, and errors for key~~many~~ variables are < 10% (Chassignet et al. 2009, Metzger et al. 2017). Local validations are reported here in Appendix Fig A1. Hindcasts differ from operational forecast simulations in that the rate of change and evolution of spatial structure is known; the rolling 5-day analysis window has overlapping temporal information to ensure a close fit to environmental conditions. This is crucial for infrequent zenith altimeter data which prescribes the currents. P~~Another key point is that p~~ost-2008 reanalysis better represents ~~characterizes~~ the nearshore oceanography due to finer microwave footprints that reach the coast.

HYCOM reanalysis fields of near-surface sea temperature, salinity, currents and mixed layer depth (MLD) are analyzed as mean maps and sections. We focus on the summer of December 2012 to February 2013, which coincides with VIIRS reflectance, Jason-1 -2 altimeter, and Ascat-A -B scatterometer coverage that better constrains the physical oceanography. Cross-correlations between the various surface ocean and atmosphere parameters are studied in this 90 day period. Other motivations for our study period include summer's marine productivity (Pfaff et al. 2019), and the variety of conditions attributable to pulsed upwelling and shelf wave events.

Insitu measurements over the coast and shelf south of Cape Town are made by numerous government agencies: South African (SA) Weather Service, Dept Environmental Affairs, Inst Marine Technology (IMT), Council~~entre~~ for Scientific and Industrial Research - Marine Division~~ept~~, SA Dept Water Affairs, SA Hydrographic Dept; with data operationally reported and subsequently archived at the SA Data Centre for Oceanography. The Univ Cape Town Oceanography Dept hosts short-term projects and regional ocean numerical modelling.

Evaluating the 'influence' of surface reports in operational data assimilation (Table 2), values of ~24% in False Bay contrast with ~90% inland. This trend continues for upper ocean T/S observations that are nearly four times greater in Table Bay than False Bay (WOA 2013). Hence our analysis of marine conditions over the shelf south of Cape Town relies more on satellite and model than in-situ observations.

Comparisons of HYCOM reanalysis ocean data with daily gauge and radiometer measurements show reasonable agreement (cf. Appendix A-1a,b) in the period 2008-2015. The sea surface height comparison has a 24% fit with discrepancies attributable to coastal tide residuals and non co-location. Sea temperatures have a 38% fit and diverge in warm spells, the model tending to over-estimate. Comparison of ECMWF-5 reanalysis and Simonstown station hourly weather data in the period Dec 12 - Feb 13 (cf. Appendix-1c,d) are good for pressure (88%) and wind speed (62%) but lower for air temperature (21%) presumably because the 0.3° reanalysis has contributions from land. Coleman (2019) reports similar validations for the summer of 2010.

The HYCOM reanalysis has limited atmospheric outputs, so to evaluate the wind circulation south of Cape Town, the WRFv3.8 model (Skamarock et al. 2008) is used to downscale ECMWF fields, as in the simulations of Coleman (2019). The WRF model resolution of 0.1º complies with the HYCOM reanalysis, and uses default schemes for boundary layer, flux transport, radiative transfer and surface coupling. We focus on the nature of horizontal flow over False Bay during summer Dec 12 - Feb 13, a period of 'near normal' climate, eg. sea level air pressure anomaly ~ 0 hPa.

Results

Summer climate and weather

We first consider the coast and climate before analyzing the shelf and ocean. Warm dry weather and sparse vegetation characterize summer (Fig 2a,b). Satellite land surface temperatures exhibit sharp gradients from the Cape Flats (40C at 34S) to cool southern coasts (25C at 34.4S), similar to Tadross et al. (2012). Little rainfall occurs in summer so terrestrial vegetation is depleted and ocean salinity is controlled by evaporation and currents, not terrestrial run-off.

Figure 2c,d illustrates the spatial pattern of ECMWF WRF-downscaled surface winds over the False Bay region in morning and afternoon. The mean southeasterly winds pass Cape Hangklip and reach 9 m/s in mid-bay. The flow acceleration is attributed to: 1. orographic channeling (Venturi effect), 2. vertical constraint by trade wind inversion, and 3. sinking motion from declining coriolis and sensible heat flux (cf. Jury and Reason 1989). Summer winds are characterized by a low-level wind jet over False Bay, seen in earlier aircraft surveys (Jury 1991), which is embedded in a shallow moist layer (cf. Appendix A-2a). Diurnal variability is of high amplitude as evident below.

Time series of CFSr2 winds over the coast and shelf (Fig 2e,f) show a meridional component that is positive and steady except for brief reversals at the end of December 2012 and February 2013. The zonal wind component is negative and fluctuating particularly in mid-January 2013. The coastal gradient is small for mean meridional flow: shelf V = 3 m/s vs coast 1.6 m/s, however the standard deviation of zonal winds is shelf U = 6.6 m/s vs coast 2 m/s. During spells of strong easterlies from transient anticyclones, the wind vorticity contribution to coastal upwelling is dominated by the gradient of $\partial U/\partial y$.

Time series of 6-hourly CFSr2 thermal variables (Fig 2-g,h) show large landair-sea differences, as expected. Coastal air temperatures fluctuate diurnally from 15-35C while shelf temperatures rise gradually from 18 to 21C over the summer. Standard deviations vary from shelf 0.4C to coast 5.7C. The landward increase of temperature drives a seabreeze contribution to the mean meridional flow. The CFSr2 surface heat fluxes show diurnal amplitude 0-300 W/m^2 over the coast, but stay in the range 50-100 W/m^2 at the shelf edge. Hence the 0.2° CFSr2 captures the coastal gradients that govern the shelf oceanography, with attributes consistent with Navgem v1.4 that underpins the HYCOM reanalysis.

LConsidering the air pressure record from the weather station in western False Bay and matching ECMWF v5 reanalysis (cf. Appendix A-1d), we note sharp dips < 1005 hPa on 27 Dec, 29 Jan, 9 Feb, and 17 Febarge swings in the meridional wind (cf. Fig 2f) are accompanied by dips in air pressure < 1005 hPa on 27 Dec, 29 Jan, 9 Feb, 17 Feb 2013, which. These identify coastal low passage associated with trapped shelf waves. In the 27 Dec and 17 Feb cases, the (station) wind reversed from 15 m/s SE (before) to 12 m/s NW (after passage of the coastal low). CFSr2 wind vorticity and sub-surface vertical motions in False Bay (pt 3) changed from -5 10^{-4} s^{-1} / +0.7 m/day (before) to +4 10^{-4} s^{-1} / -0.8 m/day (after passage of the coastal low) and (buoy) sea temperatures diropped <below 15C the following day. Yet much of the time These abrupt changes in environmental changes are inhibitedforcing are buffered in by the semi-enclosed nature of False Bay, thus sustaining productivity.

Shelf Oceanography

In this section we characterize the shelf oceanography south of Cape Town. The shelf edge has cooler waters and lower salinity due to upwelling (Fig 3a). Equatorward winds drive surface currents into False Bay, trapping a warm salty zone against the north coast >35.3 g/kg (Fig 3a), consistent with Dufois and Rouault (2012). The summer water flux is negative across the region during summer (Fig 3b), as evaporation of 4-6 mm/day exceeds precipitation of 1-2 mm/day. Fast and divergent winds dessicate the Cape Peninsula in contrast with orographic lifting over the eastern mountains. Hence the P – E field varies from neutral inside False Bay to strongly negative west of Cape Town.

False Bay has a narrow exposure to the Southern Ocean. SW swells of ~3 m tend to refract into the bay producing greater energy on the east side (Fig 3c). The ocean mixed layer depth ranges from < 10 m inside False Bay to > 50 m outside, due to kinematic exposure and thermal stratification. Mean currents (Fig 3d) are weak in the northern half of False Bay, but westward at the shelf edge and drawn into the Benguela Current.

Winds and currents are sheared into clockwise gyres that increase water residence time enabling nutrient build-up and phytoplankton blooms within False Bay (satellite-derived chlorophyll > 10 mg/m^3, Fig 3e). Month-to-month changes in productivity relate to wind angle, intensity of pulsed upwelling (cf. Appendix A-2b) and prevalence of rotary circulations.

Figure 3f presents the Dec 12 - Feb 13 sequence of monthly SST fields based on MODIS IR satellite. There is a cold upwelling plume west of Cape Town and warm waters off the shelf in Jan-Feb 13. Yet within False Bay we find subtle structures: remnants of repeated upwelling off Cape Hangklip create a cold area in the middle of the bay, while warmer waters hug the northeastern coast, beneath the wind shadow from the eastern mountains. Sustained upwelling and widespread cold SSTs in December 2012 are replaced by warm intrusions and nearshore quiescent zones by February 2013.

The Dec 12 - Feb 13 mean HYCOM depth sections on 18.6E in Figure 4a-d illustrate an upper 20 m layer with temperatures and salinity of 20C, 35.4 g/kg. Shelf-edge upwelling creates a wedge of 12C, 34.7 g/kg waters below 60 m. Zonal currents are weak inshore and strongly westward at shelf-edge above 20 m. HYCOM meridional currents reveal an overturning circulation, with deeper offshore flow and very shallow onshore flow. HYCOM daily time series at three points along 18.6E exhibit pulsing and cooler fresher conditions in the south compared with the north (Fig 4e-g). There is a strong gradient in zonal currents from –.5 m/s

Formatiert: Nicht unterstrichen

at shelf-edge to zero at the coast.

Statistical analysis is given in Table 3 and reveals that inshore (pt 1 at 34.1S) sea temperatures are more sensitive to waves than winds, and that offshore (pt 3 at 34.3S) sea temperatures follow zonal winds more than currents. We note that offshore and inshore temperatures are uncorrelated, and offshore salinity is negatively related to inshore temperature. Coastal and shelf-edge salinity are correlated, and inshore salinity responds to zonal currents (-r). HYCOM zonal currents inshore and offshore associate similarly to winds at 1-day lead, and being correlated with each other – suggest that Ekman transport frequently overrides the clockwise gyre.

Time series of Wavewatch3 swell characteristics at coast and shelf-edge virtual buoys are given in Fig 4h-j. Swell heights offshore (pt 4 at 34.4S) oscillate around 2 m except for a spell of stormy seas at the end of December 2012. Near-shore swell heights (pt 1 at 34.1S) remain near 1 m after attenuation. Southwest swell directions prevail offshore with an occasional swing to southeast. Inshore directions refract to southerly and show little change. Swell periods from 9 to 13 s tend to 'bunch' inshore < 8 s. The 25 km W3 reanalysis captures the coastal gradient in swell properties, but finer resolution or downscaling would be ideal.

This case study highlights the role played by False Bay at the interface between the Benguela and Agulhas ecosystems. Initially the bay is dominated by cool upwelling waters that are well mixed, but through the summer a warm surface layer forms near the coast – improving productivity (cf. Fig 3e). The leakage of nutrient-rich upwelled waters back into False Bay is evident (cf. Fig 4a). Stormy spells can disrupt the coastal gradient (in early January 2013, cf. Fig 4e,h) that is typical of summer.

Conclusions

Mesoscale datasets were employed to study the marine climate and physical oceanography of False Bay nearsouth of Cape Town during summer 2012-13. The 0.083° HYCOM v3.1 reanalysis offers new insights on the spatial and temporal nature of air-sea interactions, and consistently represents a coastward reduction of mixing that enhances thermal stratification (cf. Fig 3c, 4a,b). Cross-coast gradients are particularly strong for zonal wind and current, temperature and salinity, and wave height. The reanalysis circulation obtains westward flow across the mouth (–0.4 m/s) and a weak clockwise gyre in mid-bay (cf. Fig 3d) that sustain-simproves productivity (Fig 3e). The mesoscale features seen here are consistent with Coleman (2019), whose high resolution model assimilated the very same HYCOM and ECMWF-

WRF data. Under summer-time southeasterly winds, the clockwise gyre in False Bay was modelled to have inflow / outflow of ~0.2 m/s on the upper-west / lower-east side, and a sea temperature increase of ~5C from deep-offshore to surface-inshore. These features (∂V/∂z, ∂T/∂y) are reflected in the HYCOM reanalysis (cf. Fig 4d,e) and in Coleman (2019, Fig 6-22,6-26 therein). Cool nutrient-rich Benguela waters enter False Bay from its southwest corner and infiltrate the bay via the clockwise circulation (cf. Fig 3d, 4c). The cool wedge underlies a warm layer near the coast during summer (cf. Fig 4a) that improves productivity.

Temporal variability during summer is dominated by SE winds that accelerate near Cape Hangklip and fan out across False Bay, promoting dry weather. Virtual buoy time series in Dec 12 - Feb 13 exhibit weather-pulsed upwelling, and station intercomparisons build confidence that coupled reanalyses yield opportunities to study air-sea interactions in coastal zones with complex topography. Yet our 0.083° reanalysis has 16 data points in the embayment south of Cape Town. Finer downscaling could propagate ambiguities from microwave radiometers. Thus we propose that current technology allows many questions to be answered, from coastal processes to climate change. Longer summers in Cape Town could see a shift in resources from land to sea. This sentinel for global impacts on sustainable development needs on-going scientific assessment in support of holistic management.

Acknowledgements

We thank the SA Institute for Maritime Technology for provision of hourly weather station, tide gauge, and buoy data off Simonstown. The ~~1st~~ author recognizes on-going support from the SA Dept of Education. Sen Chiao of San José State Univ, CA provided the WRF downscaled wind fields.

References

Bang, N.D. 1971. The southern Benguela current region in February, 1966, Part II. Bathythermography and air-sea interactions. Deep Sea Res. 18, 209-224.

Blamey, L.K., Howard, J.A.E., Agenbag, J., Jarre, A. 2012. Regime-shifts in the southern Benguela shelf and inshore region. Prog Oceanogr. 106, 80-95.

Botes, W. 1988. Shallow water current meters comparative study: False Bay. CSIR Report T/SEA 8803, 14; Stellenbosch.

Brown, A.C., Davies, B.R., Day, J.A., Gardiner, A.J.C. 1991. Chemical pollution loading of False Bay, in Jackson, W.P.U. [ed.] False Bay 21 years on - an environmental assessment. Proc. Symposium. Trans. R. Soc. S. Afr. 47, 703-716.

Brundrit, G. 2009. Global Climate Change and Adaptation: City of Cape Town sea-level rise risk assessment, Phase 5 Full investigation of alongshore features. City of Cape Town.

Chassignet, E.P. and 18 co-authors. 2009. US GODAE: Global ocean prediction with the Hybrid coordinate ocean model (HYCOM). Oceanography 22, 64-75.

Coleman, F. 2019. The development and validation of a hydrodynamic model of False Bay, MSc thesis, Univ. Stellenbosch, 166 pp.

Cummings, J.A. and Smedstad, O.M. 2013. Variational data assimilation for the global ocean. Data Assimilation for Atmospheric, Oceanic and Hydrologic Applications vol 2, SK Park and L Xu eds., Springer-Verlag, 303-343.

Dee, D.P. and 35 co-authors 2011. The ERA-interim reanalysis: configuration and performance of the data assimilation system. Quart J Royal Meteor. Soc. 137, 553-597.

de Vos, M., Rautenbach, C. and Ansorge, I. 2014. The inshore circulation at Fish Hoek. Department of Oceanography UCT, Internal report.

Dufois, F. and Rouault, M., 2012. Sea surface temperature in False Bay (South Africa): towards a better understanding of its seasonal and inter-annual variability. Continental Shelf Res. 43, 24-35.

Engelbrecht, F., Landman, W.A., Engelbrecht, C., Landman, S., Bopape, M.M., Roux, B., McGregor, J.L. and Thatcher, M. 2011. Multi-scale climate modelling over Southern Africa using a variable-resolution global model. Water SA, 37, 647-658.

Fourie, J.P., Ansorge, I., Backeberg, B., Cawthra, H.C., MacHutchon, M.R., vanZyl, F.W. 2015. The influence of wave action on coastal erosion along Monwabisi Beach, Cape Town. S. Afr. J. Geometrics. 4, 96-109.

Giljam R. 2002. The effect of the Cape Flats aquifer on the water quality of False Bay. MSc Thesis, Univ. Cape Town.

Griffiths, C., Robinson, T., Lange, L., Mead, A. 2010. Marine biodiversity in South Africa – state of knowledge, spatial patterns and threats. PloS One 5(8): e123008.

Grundlingh, M., Hunter, I., & Potgieter, E. 1989. Bottom currents at the entrance to False Bay. Continental Shelf Research, 9, 1029-1048.

Grundlingh, M., and Largier, J. 1991. Physical oceanography of False Bay: a Review. Trans royal soc S Afr 47, 387-400.

Hughes, P. and Brundrit, G.B. 1991. The vulnerability of the False Bay coast line to the projected rise in sea level, Trans Roy Soc S Afr 47, 519-534.

Hurlburt, H.E. and 18 co-authors. 2009. High resolution global and basin-scale ocean analyses and forecasts. Oceanography 22, 110-127.

Jacobson, M., Hermes, J., Jackson-Veitch, J., & Halo, I. 2014. The influence of a spatially varying wind field on the circulation and thermal structure of False Bay during summer: a numerical modelling study. Dept Oceanography, UCT Internal Report.

Johnson H.K., Vested, H.J., Hersbach, H., Højstrup, J. and Larsen, S.E. 1999. The coupling between wind and waves in the WAM Model. J. Atmos. Oceanic Technol. 16, 1780-1790.

Joubert, J.R. and vanNiekerk, J.L. 2013. South African wave energy resource data, a case study, Stellenbosch, CRSES Internal Report, Stellenbosch.

Jury, M.R. 1991. The weather of False Bay, Trans Roy Soc S Afr 47, 401-427

Jury, M.R. and Reason, C.J., 1989. Extreme subsidence in the Agulhas-Benguela air mass transition, Bound Layer Meteorol, 46, 35-51.

Jury, M.R. and Brundrit, G.B. 1992. Temporal organisation of upwelling in the southern Benguela ecosystem by resonant coastal trapped waves in the ocean and atmosphere, S. Afr. J. Marine Science, 12, 219-224.

Largier, J.L., Chapman, P., Peterson, W.T., Swart, V.P. 1992. The Western Agulhas Bank — circulation, stratification and ecology. S Afr J Marine Sci 12: 319-339.

Lloyd, P., Plaganyi, E.E., Weeks, S.J., Magno-Canto, M. and Plaganyi, G. 2012. Ocean warming alters species abundance patterns and increases species diversity in an African subtropical reef-fish community. Fish Oceanogr. 21, 78-94.

Lutjeharms, J.R.E. and Stockton. P.L. 1991. Aspects of the upwelling regime between Cape Point and Cape Agulhas, South Africa. S Afr J Marine Sci 10: 91-102.

Mather, A., Garland, G. and Stretch, D. 2009. Southern African sea levels: corrections, influences and trends. Afr. J. Marine Science, 31, 145-156.

Metzger, E.J. and 12 co-authors. 2014. US Navy operational global ocean and Arctic ice prediction systems. Oceanography 27, 32-43.

Metzger, E.J., Helber, R.W., Hogan, P.J., Posey, P.G., Thoppil, P.G., Townsend, T.L., Wallcraft, A.J., Smedstad, O.M., Franklin, D.S., Zamudio-Lopez, L. and Phelps, M.W. 2017. (HYCOM-NCODA) Global Ocean Forecast System 3.1 validation testing, NRL/MR/7320-17-9722, <www7320.nrlssc.navy.mil/pubs/2017/metzger-2017.pdf>

Nelson, G., Cooper, R.M., and Cruickshank, S. 1991. Time series from a current meter array near Cape Point, Trans Roy Soc S Afr 47, 471-482.

Nicholson, S.A. 2011. The circulation and thermal structure of False Bay: a process-oriented numerical modelling and observational study, MSc Thesis. Dept. Physical Oceanography, Univ. Cape Town.

Parsons, R.P. 2000. Assessment of the impact of the Cape Flats on surrounding water bodies. S. Peninsula Muni. Report 074/SPM-1, Somerset West.

Penven, P., Brundrit, G.B., deVerdiere, C.A., Freon, P., Johnson, A.S., and Shillington, F.A. 2001. A regional hydrodynamic model of upwelling in the Southern Benguela. S. African J. Science 97, 472-475.

Pfaff, M.C., and 31 coauthors. 2019. A synthesis of three decades of socio-ecological change in False Bay, South Africa: setting the scene for multidisciplinary research and management. Elem Sci Anth, 7: 32. doi.org/10.1525/elementa.367

Rautenbach, C. 2014. The influence of a space varying wind field on wind-wave generation in False Bay, South Africa. SAMSS conference. Stellenbosch.

Reynolds, R.W., Rayner, N.A., Smith, T.M., Stokes, D.C., and Wang, W. 2002. An improved in situ and satellite SST analysis for climate. J Climate 15, 1609-1625.

Rouault, M., Pohl, B. and Penven, P. 2010. Coastal oceanic climate change and variability from 1982 to 2009 around South Africa. Afr. J. Marine Science, 32, 237-246.

Roux, G.B. & Toms, G. 2013. Reduction of seawall overtopping at the Strand. Stellenbosch University, Internal Report.

Saha, S. and 18 co-authors. 2014. The NCEP Climate Forecast System version 2. J. Climate, 27, 2185-2208.

Schlegel, R.W., Oliver, E.C., Wernberg, T., Smit, A.J. 2017. Nearshore and offshore cooccurrence of marine heatwaves and cold-spells. Prog Oceanogr. 151, 189-205.

Schilperoort, D.E., Shillington, F., Hermes, J., and Rautenbach, C. 2013. Investigation into the capability of the Conformal-Cubic Atmospheric Model in representing the wind fields and patterns over the Fasle Bay region in comparison to NCEP/NCAR and observational data. Department of Oceanography, UCT Internal Report.

Shannon, L.V. [ed.] 1985. South African Ocean Colour and Upwelling Experiment, Sea Fisheries Research Institute, Cape Town, 270 pp.

Shannon, L.V. and Field, J.G. 1985. Are fish stocks food-limited in the Southern Benguela pelagic ecosystem? Mar Ecol Prog Ser 22(1), 7-19. doi:10.3354/meps022007.

Skamarock, W.C., Klemp, J.B.. Dudhia, J., Gill, D.O., Barker, D.M., Huang, X., Wang, W. and Powers, J.G. 2008. A description of the Advanced Research WRF v3. NCAR Tech Note, 475 pp.

Tadross, M.A., Taylor, A., and Johnston, P.A. 2012. Understanding Cape Town's climate. In: Cartwright, A, Oelofse, G, Parnell, S, Ward, S. (eds) Climate change at the city scale: impacts, mitigation and adaptation in Cape Town, Routledge, 9-20.

Taljaard, S. 1991. The origin and distribution of dissolved nutrients in False Bay. Royal Society of South Africa Transactions TRSAAC 47(4/5).

Taljaard, S., van Ballegooyen, R. and Morant, P. 2000. False Bay Water Quality Review. CSIR Report ENV-SC 86: 2, Stellenbosch.

Theron, A., Rossouw, M., Barwell, L., Maherry, A., Diedericks, G., & de Wet, P. 2010. Quantification of risk to coastal areas and development: wave run-up and erosion. Sceince real and relevant conference. Pretoria: CSIR Internal Report.

Theron, A., Rossouw, M., Rautenbach, C., vonSaint Ange, U., Maherry, A., & August, M. 2014. Determination of inshore wave climate along South African coast: phase 1 coastal hazard and vulnerability assessment. Stellenbosch: CSIR Internal Report.

Theron, A., Rossouw, M., Rautenbach, C., van Niekerk, L., Luck-Vogel, M., & Cilliers, L. 2014. South African coastal vulnerability assessment: phase 2. Stellenbosch: CSIR internal report.

Tolman, H.L. 2002. User manual and system documentation of WAVEWATCH-III version 2.22. NCEP Tech. Note, Washington, 139 pp.

vanBallegooyen, R. 1991. The dynamics relevant to the modelling of synoptic scale circulations within False Bay. Trans royal soc S Afr 47, 419-431.

Wainman, C.K., Polito, A., Nelson, G. 1987. Winds and subsurface currents in the False bay region, South Africa. S. Afr. J. Marine Science 5: 337-346.

World Ocean Atlas. 2013. Locarnini, R.A. , Zweng, M.M. and 11 co-authors: Temperature / Salinity, NOAA Atlas NESDIS 73 / 74, 40 / 39 pp. (observation density).

Table 1

ACRONYM	NAME	SOURCE
ASCAT	Advanced Scatterometer Reanalysis	Univ Hawaii APDRC
CFSr2	Coupled Forecast System v2 reanalysis	Univ Hawaii APDRC
CHIRPS	Climate Hazards InfraRed Precipitation with Station v2	UCB via IRI Clim.Library
ECMWF	European Centre for Medium-Range Weather Forecasts v5	Climate Explorer
HYCOM	Hybrid Coordinate Ocean Model v3.1 reanalysis	Univ Hawaii APDRC
IMT	Institute for Maritime Technology of South Africa	Station data on request
MADIS	Meteorological Assimilation and Data Ingest System	NCEP
MODIS	Moderate imaging Infrared Spectrometer	USGS via IRI Clim.Library
NASA	National Aeronautics and Space Administration	NASA-giovanni
NAVGEM	US Navy global environmental model v1.4	Coastwatch Erddap
NOAA	National Oceanic and Atmospheric Administration	NOAA via IRI Clim.Library
VIIRS	Visible Infrared Imaging Radiometer Suite	Coastwatch Erddap
W3	Wavewatch v3 ocean swell reanalysis	Univ Hawaii APDRC

HYCOM information:
www.hycom.org/hycom/documentation
Satellite information:
www.wmo-sat.info/oscar/gapanalyses?mission=12
www.wmo-sat.info/oscar/gapanalyses?mission=13
www.wmo-sat.info/oscar/gapanalyses?variable=133
www.wmo-sat.info/oscar/gapanalyses?variable=148

Table 2: Relative influence of surface weather observations in model assimilation, with grey land mask. Stations reporting (in 2020): land-based private ○ official ● , marine-based on-line ✔ off-line ✖ . Curved line is routine aircraft wind / temp profile; sources: NASA, NO-AA, MADIS, Wundermap.

33.85S	0.91	0.92	0.92	0.92	0.92	0.94	0.95	0.96	1.05
33.95S	0.88	0.94	0.89	0.89	0.89	0.90	0.91	0.91	1.03
34.05S	0.42	0.38	0.34	0.28	0.28	0.28	0.31	0.37	0.78
34.15S	0.40	0.34	0.31	0.24	0.24	0.24	0.28	0.31	0.77
34.25S	0.34	0.33	0.30	0.21	0.21	0.24	0.26	0.28	0.76
34.35S	0.34	0.30	0.27	0.24	0.24	0.19	0.22	0.26	0.74
34.45S	0.30	0.30	0.21	0.16	0.16	0.18	0.22	0.25	0.62
34.55S	0.15	0.16	0.15	0.16	0.16	0.16	0.18	0.22	0.50
lat / lon	18.25E	18.35E	18.45E	18.55E	18.65E	18.75E	18.85E	18.95E	19.05E

Table 3: Correlation of daily time series in the period December 2012 to February 2013: HYCOM surface layer temperature T, salinity S and zonal current Uc (pt 1, 3; cf. Fig 4a), ASCAT wind U V components (pt 2) at 1-day lead and W3 swell height (pt 4). Values > |0.27| are significant at 90% confidence (bold) with ~40 degrees of freedom.

N=89	T1	T3	S1	S3	Uc1	Uc3	V-1	U-1
T3	0.02							
S1	-0.14	0.26						
S3	**-0.43**	**0.74**	**0.56**					
Uc1	0.06	0.16	-0.26	0.00				
Uc3	0.08	0.13	-0.25	-0.02	**0.96**			
V-1	-0.03	-0.05	0.26	0.06	**-0.68**	**-0.78**		
U-1	0.08	**0.33**	-0.14	0.12	**0.68**	**0.72**	**-0.56**	
swell4	**-0.31**	0.00	-0.12	0.10	-0.10	-0.11	0.10	-0.10

FIGURES

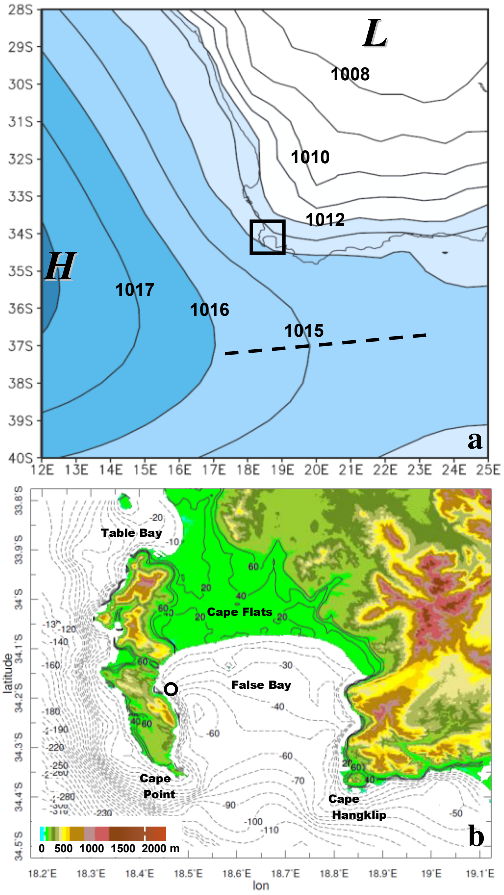

Fig 1 (a) Mean sea level air pressure in summer Dec 12 to Feb 13, box = False Bay area, dashed = subtropical ridge. (b) Topography (shading) and bathymetry contours; place names are labelled, dot is the IMT buoy / tide gauge / weather station off Simonstown.

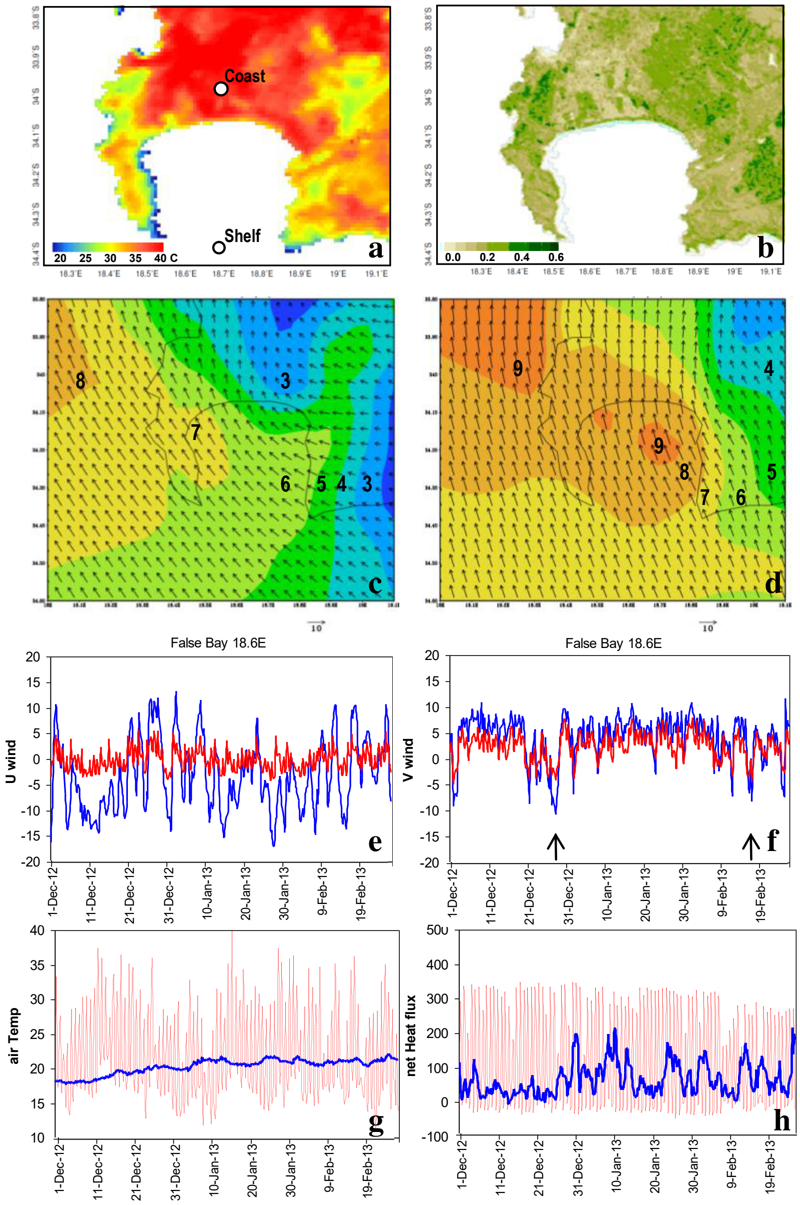

Fig 2 Mean conditions for summer Dec 12 – Feb 13: (a) MODIS 1 km day-time land temperature and (b) vegetation fraction. WRF-downscaled wind vectors and speed (shaded m/s) for Dec 12 – Feb 13: (c) 08:00 morning, (d) 14:00 afternoon. Time series Dec 12 – Feb 13 of 6-hourly CFSr2 data at shelf-edge (blue, sea) and coast (red, land): (e) U wind, (f) V wind, (g) air temperature, and (h) net heat flux. Arrows in (f) refer to coastal low/shelf wave passage noted in text.

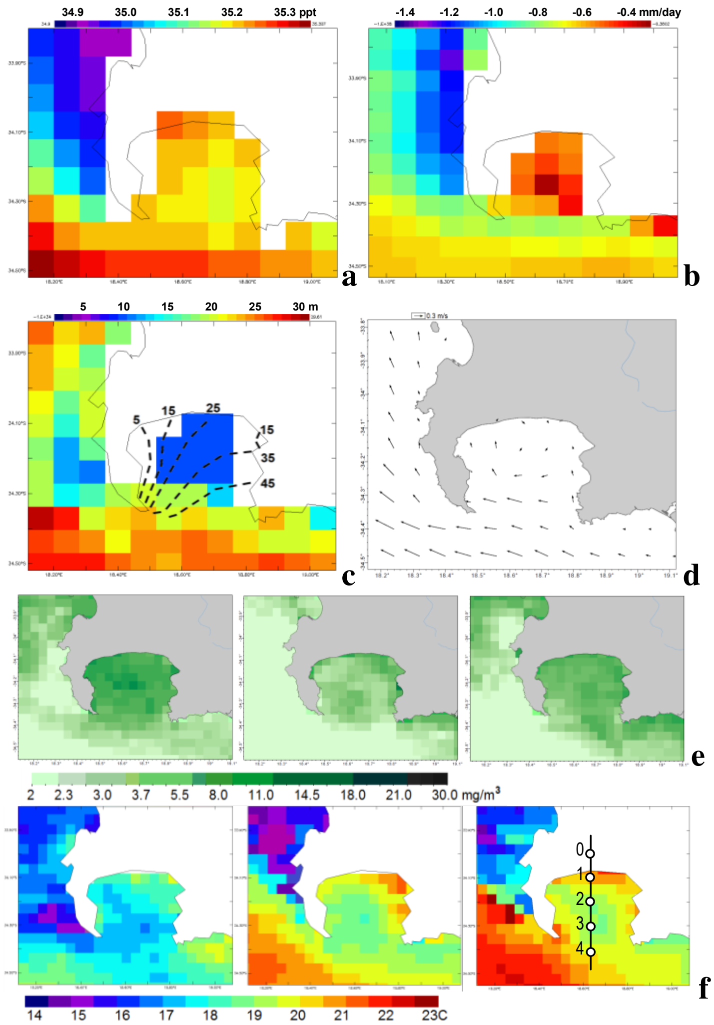

Fig 3 Mean ocean conditions for summer Dec 12 – Feb 13 from HYCOM hindcast: (a) 2 m salinity, (b) precipitation - evaporation balance, (c) mixed layer depth (m), and wave energy isolines (kW/m, after Joubert and vanNiekerk 2013) and (d) 6 m currents; with raster shading at native resolution. Sequences of Dec 12 (left) to Feb 13 monthly 4 km satellite: (e) VIIRS ocean color (derived chlorophyll), and (f) MODIS sea surface temperature (C). Points in (f) indicate virtual stations for time series, Table 2 statistics, and the depth section in Fig 4a-d.

40
60
80
100

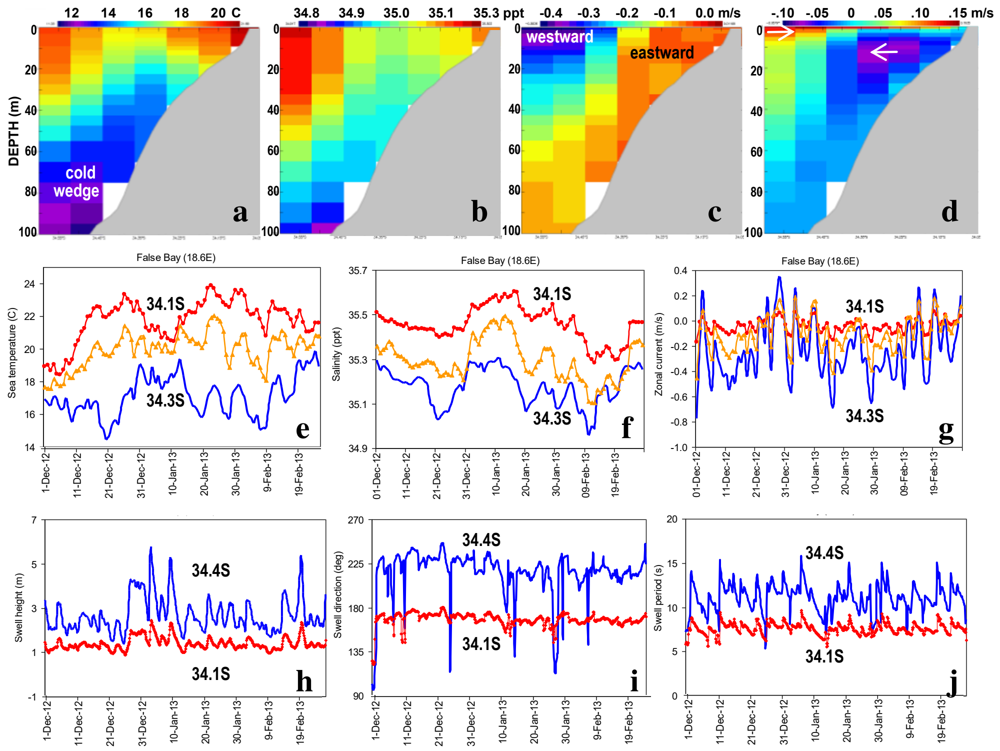

Fig 4 HYCOM mean summer Dec 12 – Feb 13 depth section along 18.6E: (a) temperature, (b) salinity, (c) zonal current, (d) meridional current; with shelf profile. (e,f,g) Surface layer T, S, U time series at points 1-3. Ocean wave time series Dec 12 – Feb 13 from W3 data at pts 1, 4: (h) swell height, (i) swell direction, (j) swell period. Shelf-edge is plotted –blue, mid-bay –orange, coastal –red.

Appendix

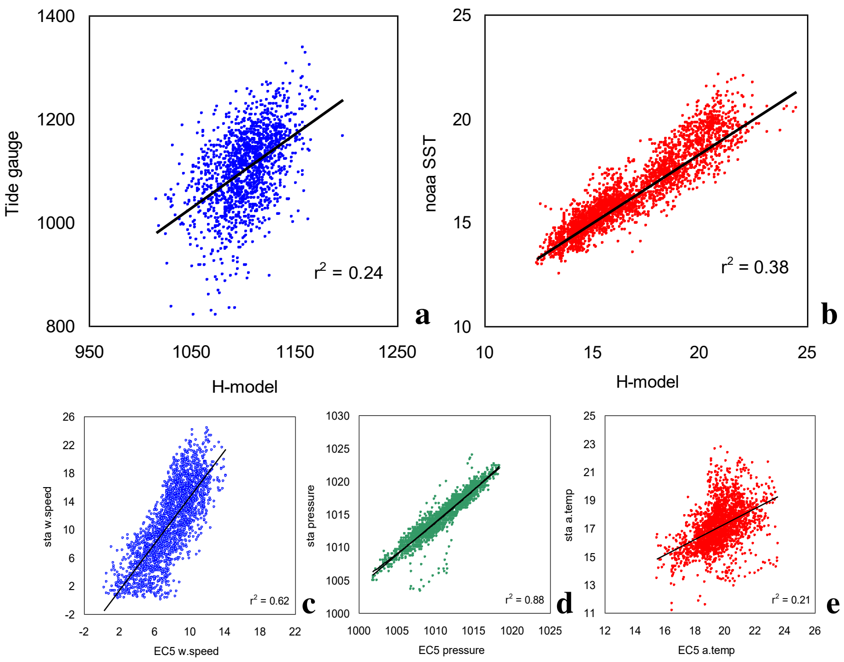

A-1 Comparison of daily HYCOM model at nearest grid-point and: (a) sea surface height from tide gauge off Simonstown in western False Bay (cf. Fig 1b) and (b) sea surface temperature from NOAA satellite; 2008-2015. Lower: Comparison of hourly ECMWF v5 reanalysis at nearest grid-point and weather station observation off Simonstown in western False Bay, 1 Dec 12 – 28 Feb 13: c) wind speed, d) pressure, and e) air temperature.

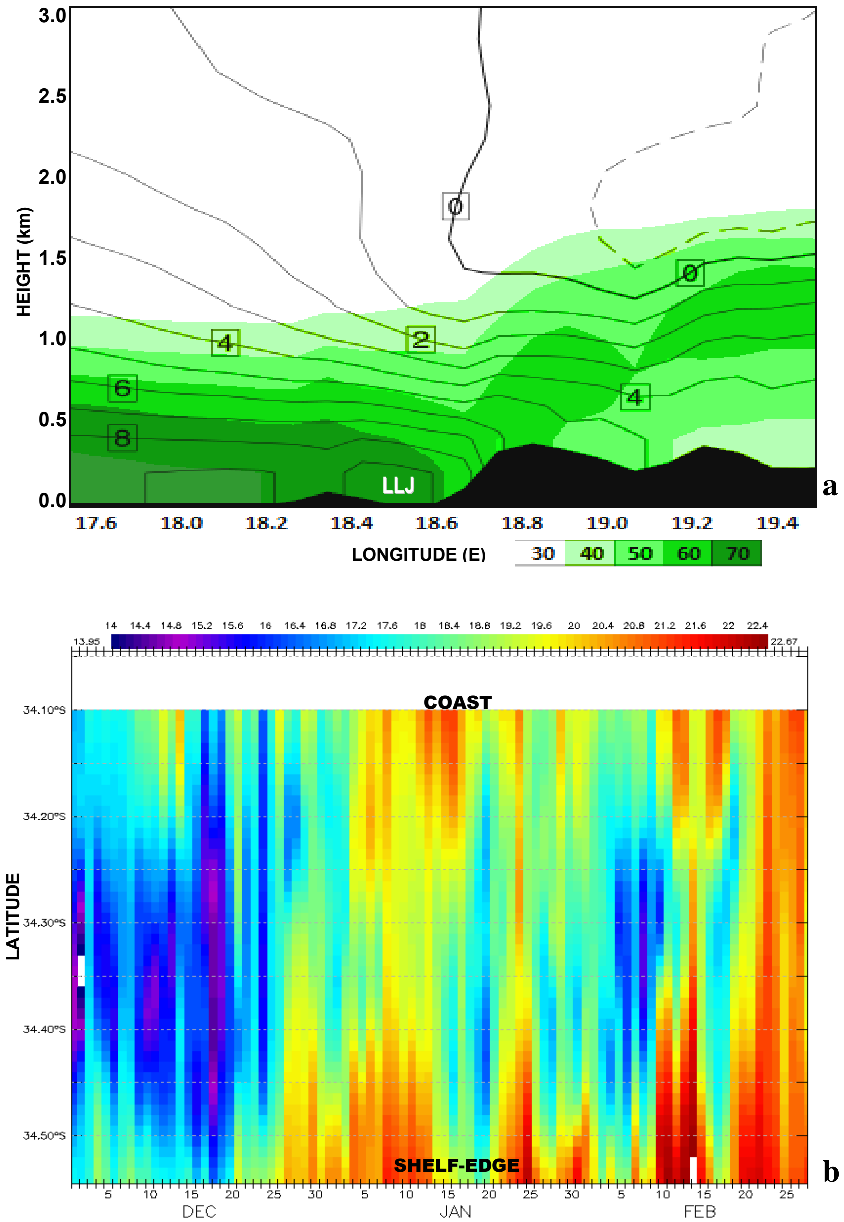

A-2 a) down-scaled WRF meridional wind isotachs and humidity % (shaded) in Dec 12 – Feb 13, plotted in vertical section on 34.1S, identifying the shallowness of equatorward flow, corresponding with Fig 2c,d. b) Hovmoller plot of daily 1 km SST on 18.6E, assimilated by GHR L4 satellite product, along the same line as Fig 4.